coatings

MDPI

Article

Joining Superconducting MgB_2 Parts by Spark Plasma Sintering: A New Technique with High Potential for Manufacturing Future Superconducting Devices

Yohann Thimont [1], Yiteng Xing [2,3], Pierre Bernstein [2], Muralidhar Miryala [3] and Jacques Noudem [2,*]

[1] CIRIMAT, Université de Toulouse, CNRS, INPT, UPS, 118 Route de Narbonne, 31062 Toulouse, France
[2] Normandie University, ENSICAEN, UNICAEN, CNRS, CRISMAT, 14000 Caen, France
[3] Materials for Energy and Environmental Laboratory, Superconducting Materials Group, Graduate School of Science & Engineering, Shibaura Institute of Technology, 3-7-5 Toyosu, Koto-ku, Tokyo 135-8548, Japan
* Correspondence: jacques.noudem@ensicaen.fr

Abstract: MgB_2 pellets that were sintered by Spark Plasma Sintering (SPS) from commercial MgB_2 powder were soldered by a SPS process and compared to unsoldered ones. The soldered samples were characterized by scanning and transmission electron microscopy which have shown no visible defects at the junction. SQUID magnetometry and four probes resistance measurements have confirmed that the soldered pellets present the same magnetic properties as the unsoldered ones. The presented soldering technique could find applications for manufacturing superconducting devices with custom shapes which could be used as rotors for motors and generators, magnets and magnetic shields. This new approach could generate a high potential interest for industrials in these and connected domains such as the development of new electrical planes using superconducting technologies.

Keywords: MgB_2; bulk; superconductor; soldering; Spark Plasma Sintering

check for updates

Citation: Thimont, Y.; Xing, Y.; Bernstein, P.; Miryala, M.; Noudem, J. Joining Superconducting MgB_2 Parts by Spark Plasma Sintering: A New Technique with High Potential for Manufacturing Future Superconducting Devices. *Coatings* **2022**, *12*, 1151. https://doi.org/10.3390/coatings12081151

Academic Editor: Devis Bellucci

Received: 27 June 2022
Accepted: 5 August 2022
Published: 9 August 2022

Publisher's Note: MDPI stays neutral with regard to jurisdictional claims in published maps and institutional affiliations.

Copyright: © 2022 by the authors. Licensee MDPI, Basel, Switzerland. This article is an open access article distributed under the terms and conditions of the Creative Commons Attribution (CC BY) license (https://creativecommons.org/licenses/by/4.0/).

1. Introduction

Magnesium Diboride (MgB_2) is an intermetallic material whose structure consist of stacked magnesium planes alternating with boron planes along the *c* axis. Each plane is arranged according to a 2D hexagonal lattice. While this compound has been known since the 1950s, its superconductivity was only discovered in 2001. Its critical temperature is T_c = 39 K [1,2] and it shows a high critical current density ($J_c = 10^6$ A/cm^2 at 10 K in zero field for the bulk material [3,4]). While thin films [5] and powders [6] show anisotropic superconducting properties, sintered ceramics are isotropic. One of the main advantages of MgB_2 is its simple stoichiometry in opposition to that of high temperature oxide superconductors such as $YBa_2Cu_3O_7$, the superconducting properties of which are strongly dependent on the oxygen content [7]. It includes cheap and non-toxic elements and shows a high mechanical hardness of about 12.5 GPa [8]. As a consequence, MgB_2 could be advantageously used in devices cooled with liquid hydrogen, especially superconducting motors and generators or for fabricating magnets, magnetic shields and MRI superconducting coils [9]. However, as a consequence of its strong hardness, machining it is difficult, which limits the development of applications. In this paper we report the properties of MgB_2 samples that were soldered using the Spark Plasma Sintering (SPS) [10] technique. SPS is currently used for sintering pellets, although rarely in reactive mode and more rarely for the direct fabrication of complex shapes by sacrificial materials [11]. Otherwise, few studies report joining two similar parts of the same material or of different materials by SPS (see [12,13]). This route for soldering MgB_2 bulks could help the development of superconducting devices with complex shapes by soldering smaller parts between them. This very innovative approach could overcome some limitations to fabricate new devices. In this case, different superconducting shapes could emerge in the future for specific applications

like magnetic screening, superconductor motors and generators in various domains such as the development of electrical aircrafts which is one of the challenges of our society [14].

2. Experimental Details

A schema of the experimental procedure is reported in Figure 1. A commercial MgB_2 powder (99.9% purity, PAVEZYUM advanced Chemicals, Gebze Kocaeli, Turkey) was introduced in a SPS die covered with a 1 µm thick Papyex foil. The powder was pressed at 50 MPa in primary vacuum while applying for 30 min a pulsed current large enough for heating it at 1050 °C [15], (FCT Systeme GmbH, HD25, Rauenstein, Germany). After cooling it down in primary vacuum, the sintered pellet was extracted from the SPS die and mirror polished in pure ethanol. Its density was 95% of the theoretical value measured using the Archimedes method with ethanol. The pellet was cut in three parts using a diamond disc lubricated with pure ethanol. The surface of the obtained parts was mirror polished with a 1/1200 sand disc in pure ethanol. Two of the polished parts were staked in the SPS die. The same sintering process as for the pellet fabrication was applied and the two stacked parts were removed from the die. The molded sample showed good mechanical properties even across the soldered junction. It was cut as shown in Figure 1 in order to make available several samples for the characterization steps. The structure and microstructure were analyzed by Scanning Electron Microscopy (SEM, Caen, France) in the secondary electron mode with a ZEISS MICROSCOPE and with a JEOL 2010 Transmission Electron Microscope (TEM, Caen, France) in image and diffraction modes operated at 200 kV. The electrical resistance across the samples junctions was measured as a function of temperature in a Quantum Design Physical Properties Measurement System (PPMS, Caen, France). The magnetic moment was measured with a Superconducting Quantum Interference Device (SQUID, Caen, France) magnetometer as a function of the temperature and compared to that of an unsoldered sample with the same dimensions.

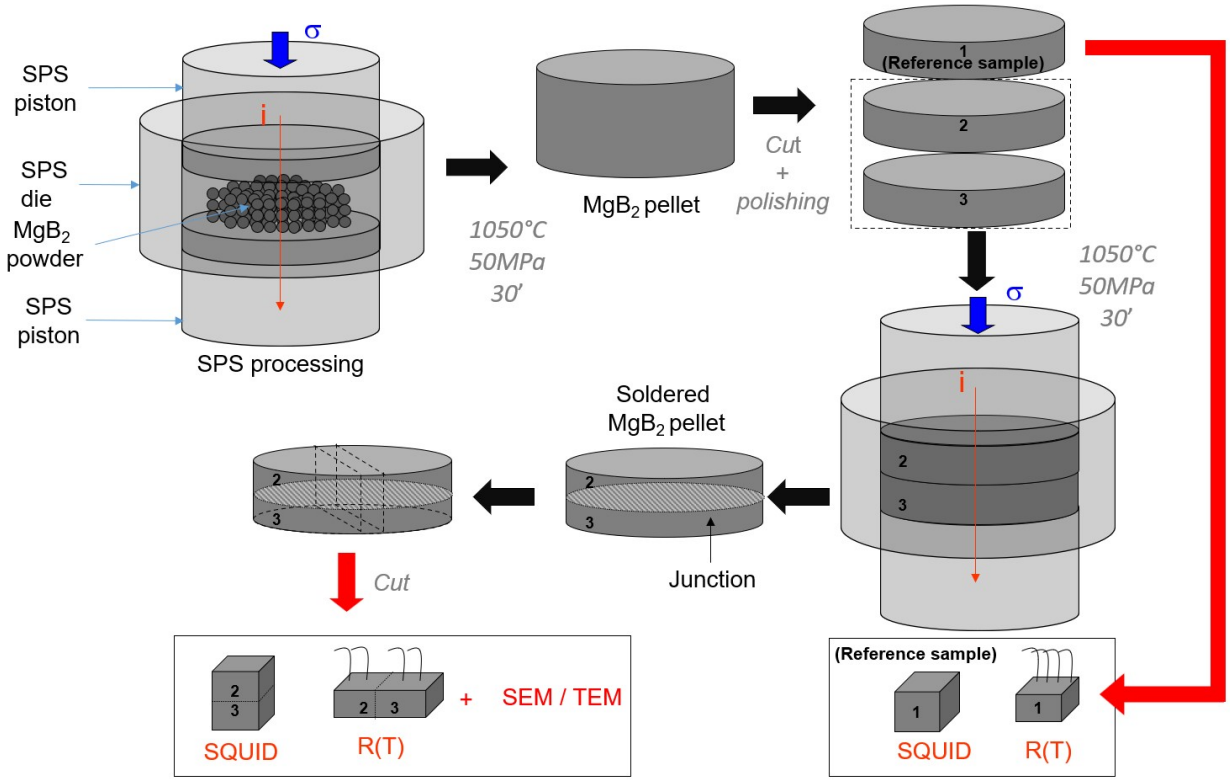

Figure 1. Schematic of the Sintering step then soldering process and soldered samples preparation for analysis.

3. Results and Discussions

(a) Microstructural and structural properties of the joined domain

A SEM (in a secondary electron mode) micrography of the interface is reported in Figure 2. Neither cracks nor porosities with a micronic size are visible. This is the evidence of an effective joining between the soldered parts, which also explains the good mechanical properties of the sample. No sign of pollutants has been found by EDX analysis. A cross section has been prepared by mechanical grinding and ionic etching. The left side of Figure 3 shows the TEM image (obtained with a JEOL 2010 MET at 200 kV) at the end of the junction. The MgB_2 grains located on both sides are in contact. The right side of Figure 3 shows an electronic diffraction pattern corresponding to the (hk0)* plane of a crystallite located at the interface. It presents the typical hexagonal MgB_2 structure, confirming that the soldering process does not change the structure of the material.

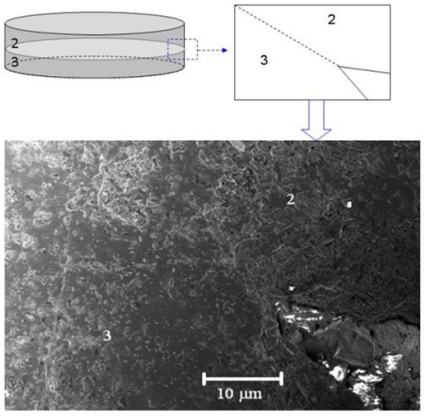

Figure 2. SEM micrography of the MgB_2 along the joined junction.

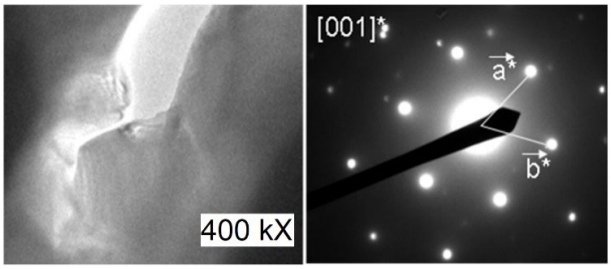

Figure 3. (**Left**) TEM micrography of the MgB_2 along the soldered junction in image mode. (**Right**) Electronic diffraction pattern of the MgB_2 crystallite showed in the micrography.

(b) Physical properties

The reference sample and two soldered samples with neighboring thicknesses were glued on a PPMS sample holder (Quantum Design). The samples were connected to the PPMS gold pads with a 20 µm aluminum wire (see Figure 4b). Their resistance was measured by the four probes technique between 5 K and 140 K (Figure 4a). The dimensions of the samples and the distance between the voltage probes are reported in Table 1. The resistivity measurements were repeated on another soldered specimen (sample n3) to check the reproducibility. The resistivity bars cut at the center and along the edge of the pellet were measured (see Figure 4d). The results are reported in Figure 4c. The welded and the unwelded parts of all the samples have turned out to be superconducting. Otherwise, the normal state resistivities are similar. The critical temperature of all the samples was equal to 38 K, which means that neither the soldering process nor the presence of the joining interface induced any degradation of the critical temperature. The magnetic moments of a soldered and a non-soldered (as a reference) sample were measured between 10 K and 40 K with a SQUID magnetometer, while applying a 2 mT field. The dimensions of the samples

are reported in Figure 5. The samples show almost the same T_c and magnetic moment, which, since they have almost the same dimensions, indicates that their properties and their shielding current lines are similar. This is only possible if the soldering plane is totally transparent to the superconducting currents and if it does not cause a limitation to the critical current density.

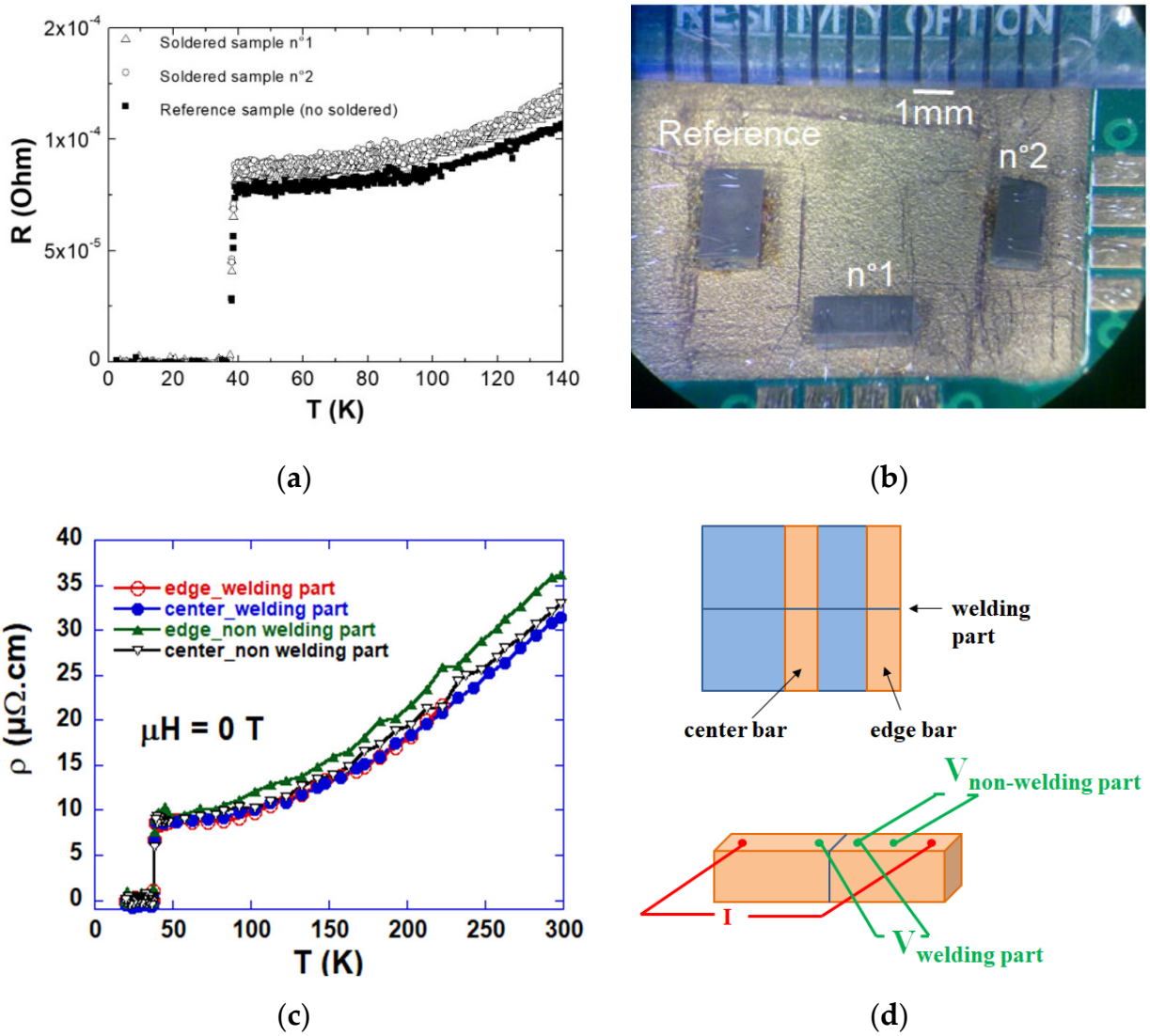

Figure 4. (**a**) Four probes measurement across the soldered junction of the sample n1 and n2 and the reference sample (without solder). (**b**) Four probes measurement device of the samples. (**c**) ρ (T) of the both welded and unwelded parts of sample 3. (**d**) The schema of the bars cut from the soldered pellet.

Table 1. Samples sizes and the distances between V+ and V− electrodes for each sample.

	D (Between V Electrodes) (mm)	Length (mm)	Width (mm)	High (mm)
Reference	1.87	2.82	1.65	1.63
n1	1.91	2.88	1.206	1.63
n2	1.34	2.58	1.43	1.56

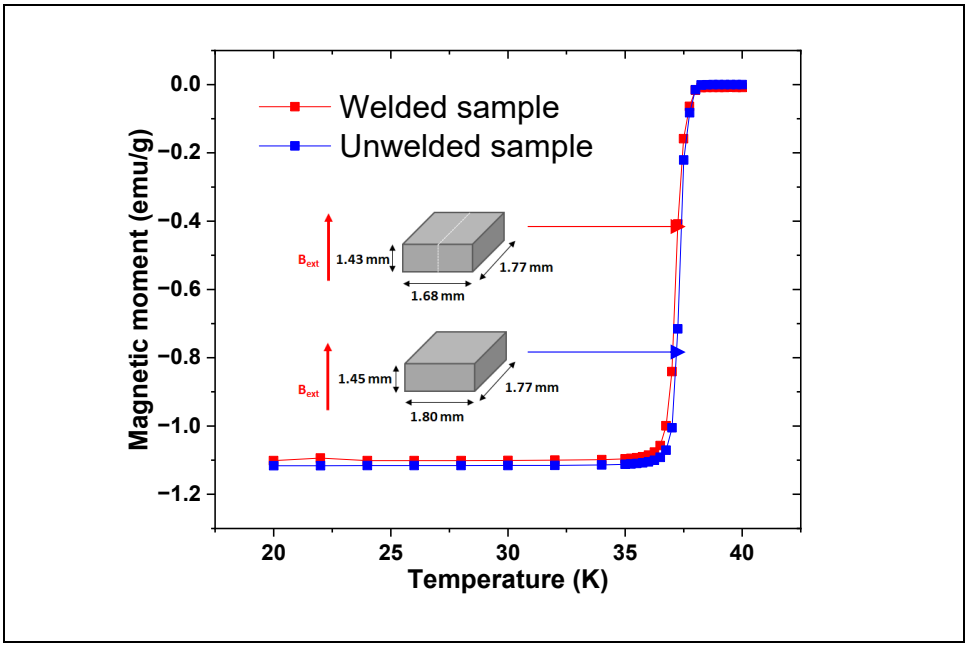

Figure 5. Magnetic moment of the unwelded and welded samples as function of the temperature.

4. Conclusions

In this article, the possibility to join different MgB_2 superconductor parts by the Spark Plasma Sintering technique was investigated.

- This procedure induces no changes in the structural and microstructural properties of the samples. The soldered junction could not be discriminated from other locations in the sample by SEM imaging, demonstrating a good matching between the welded parts.
- The critical temperature of the soldered sample was the same as that of the unsoldered ones.
- Soldered and unsoldered samples have shown the same magnetic moment below T_c, suggesting that the superconducting currents can go through the soldering plane without degradation of the critical current density.

The presented technique could be applied for developing superconducting coils, motors, magnetic shields and other applications based on the superconducting properties of MgB_2.

Author Contributions: Conceptualization, Y.T., P.B. and J.N.; methodology, Y.T., Y.X., M.M., P.B., J.N.; validation, Y.T., P.B. and J.N.; formal analysis, Y.T., Y.X. and M.M.; investigation, Y.X., M.M., Y.T., P.B. and J.N.; writing—original draft preparation, Y.T., P.B. and J.N.; writing—review and editing, Y.T., P.B. and J.N.; visualization, Y.T., Y.X., M.M., P.B. and J.N.; supervision, J.N.; project administration, J.N. All authors have read and agreed to the published version of the manuscript.

Funding: This research received no external funding.

Institutional Review Board Statement: Not applicable.

Informed Consent Statement: Not applicable.

Data Availability Statement: Data sharing is not applicable to this article.

Acknowledgments: Y.X. thanks the "Conseil Régional-Normandie, France" for her thesis grant. This work was partly supported by Shibaura Institute of Technology (SIT) International Research Center for Green Electronics.

Conflicts of Interest: The authors declare no conflict of interest.

References

1. Akimitsu, J. Symposium on Transition Metal Oxides. In Proceedings of the Spintronics IX, Sendai, Japan, 10 January 2001.
2. Nagamatsu, J.; Nakagawa, N.; Muranaka, T.; Zenitani, Y.; Akimitsu, J. Superconductivity at 39 K in magnesium diboride. *Nature* **2001**, *410*, 63–64. [CrossRef] [PubMed]
3. Kang, W.N.; Kim, M.S.; Jung, C.U.; Kim, H.J.; Choi, E.M.; Park, M.S.; Lee, S.I. Origin of the high DC transport critical current density for the MgB_2 superconductor. *arXiv* **2001**, arXiv:cond-mat/0103176.
4. Dhalle, M.; Toulemonde, P.; Beneduce, C.; Musolino, N.; Decroux, M.; Flukiger, R. Transport and inductive critical current densities in superconducting MgB_2. *Phys. C Supercond.* **2001**, *363*, 155–165. [CrossRef]
5. Ferdeghini, C.; Ferrando, V.; Grassano, G.; Ramadan, W.; Bellingeri, E.; Braccini, V.; Marre, D.; Putti, M.; Manfrinetti, P.; Palenzona, A.; et al. Kinetics of Biomass Thermal Decomposition. *Chem. Pap.* **2002**, *56*, 378–381.
6. Bud'ko, S.L.; Kogan, V.G.; Canfield, P.C. Determination of superconducting anisotropy from magnetization data on random powders as applied to $LuNi_2B_2C$, YNi_2B_2C, and MgB_2. *Phys. Rev. B* **2001**, *64*, 180506. [CrossRef]
7. Bernstein, P.; Mosqueira, J.; Siejka, J.; Vidal, F.; Thimont, Y.; McLoughlin, C.; Ferro, G. Measurements of the surface critical current of $YBa_2Cu_3O_{7-\delta}$ thin films: Probing the nonuniformity of their superconducting critical temperature along the c-axis. *J. Appl. Phys.* **2010**, *107*, 123901. [CrossRef]
8. Prikhna, T.; Gawalek, W.; Novikov, N.; Savchuk, Y.; Moshchil, V.; Sergienko, N.; Wendt, M.; Dub, S.; Melnikov, V.; Surzhenko, A.; et al. High pressure synthesis and sintering of MgB_2. *IEEE Trans. Appl. Supercond.* **2003**, *13*, 3506–3509. [CrossRef]
9. Yao, W.; Bascuñán, J.; Hahn, S.; IwasaI, Y. MgB_2 Coils for MRI Applications. *IEEE Trans. Appl. Supercond.* **2010**, *20*, 756–759. [CrossRef] [PubMed]
10. Suarez, M.; Fernandes, A.; Menendez, J.L.; Torrecillas, R.; Kessel, H.U.; Hennicke, J.; Kirchner, R.; Kessel, T. Challenges and Opportunities for Spark Plasma Sintering: A Key Technology for a New Generation of Materials. In *Sintering Applications*; IntechOpen: London, UK, 2013. [CrossRef]
11. Manière, C.; Durand, L.; Weibel, A.; Chevallier, G.; Estournes, C. A sacrificial material approach for spark plasma sintering of complex shapes. *Scr. Mater.* **2016**, *124*, 126–128. [CrossRef]
12. Hughes, L.A.; van Benthem, K. Spark Plasma Sintering Apparatus Used for the Formation of Strontium Titanate Bicrystals. *J. Vis. Exp.* **2017**, *120*, 55223. [CrossRef] [PubMed]
13. Liu, W.; Naka, M. In situ joining of dissimilar nanocrystalline materials by spark plasma sintering. *Scr. Mater.* **2003**, *48*, 1225–1230. [CrossRef]
14. Prikhna, T.; Gawalek, W.; Eisterer, M.; Weber, H.W.; Monastyrov, M.; Sokolovsky, V.; Noudem, J.; Moshchil, V.; Karpets, M.; Kovylaev, V.; et al. The effect of high-pressure synthesis on flux pinning in MgB_2-based. *Phys. C Supercond.* **2012**, *479*, 111–114. [CrossRef]
15. Noudem, J.G.; Aburras, M.; Bernstein, P.; Chaud, X.; Muralidhar, M.; Murakami, M. Development in processing of MgB_2 cryo-magnet superconductors. *J. Appl. Phys.* **2014**, *116*, 163916. [CrossRef]